Mechanism of bi-stability: tonic spiking and bursting in a neuron model

Andrey Shilnikov*
Department of Mathematics and Statistics, Georgia State University, Atlanta, GA 30303, USA

Ronald L. Calabrese and Gennady Cymbalyuk†
Biology Department, Emory University, Atlanta, GA 30322, USA
(Dated: January 28, 2004)

Neurons can demonstrate various types of activity; tonically spiking, bursting as well as silent neurons are frequently observed in electrophysiological experiments. The methods of qualitative theory of slow-fast systems applied to biophysically realistic neuron models can describe basic scenarios of how these regimes of activity can be generated and transitions between them can be made. Here we demonstrate that a bifurcation of a codimension one can explain a transition between tonic spiking behavior and bursting behavior. Namely, we argue that the Lukyanov-Shilnikov bifurcation of a saddle-node periodic orbit with non-central homoclinics is behind the phenomena of bi-stability observed in a model of a leech heart interneuron under defined pharmacological conditions. This model can exhibit two coexisting types of oscillations: tonic spiking and bursting with a large amplitude. Which regime occurs depends on the initial state of the neuron model. Moreover, the neuron model also generates weakly chaotic bursts when a control parameter is close to the bifurcation value.

PACS numbers: 02.40.Xx, 05.45.-a, 05.45.Ac, 05.45.Pq, 87.19.La

I. INTRODUCTION

Neurons are observed in one of three fundamental, generally defined modes: silence, tonic spiking and bursting. The functional role of bursting has been actively discussed in recent theoretical and experimental studies. There is agreement that it is an important mode for control of rhythmic movements and is frequently observed in central pattern generators, neuronal networks controlling motor behavior [23]. Also, bursting has been widely observed in sleep and pathological brain states [31]. More recently bursting has begun to be identified with other functions. It has been proposed to improve reliability of memory formation [18, 20]. Neurons in bursting mode differ from neurons in tonic spiking mode in their ability to transmit information and to respond to stimulation and appear to play an important role in information transfer and processing in normal states of the nervous system [13, 26]. The co-existence of bursting tonic spiking modes and of different bursting modes with each other has been observed in modeling [3–6, 8] and experimental [16, 19, 33] studies and this complexity adds potential flexibility to the nervous system. Such multistability may be controlled by neuromodulators and thus reflect the functional state of the nervous system. Multistability has many potential implications for dynamical memory and information processing in a neuron [5, 6, 22, 33, 35].

Living neurons exhibit a plethora of dynamical regimes; in addition to tonic spiking and bursting they undergo subthreshold oscillations which can be both regular or irregular or may reside in various stationary states. A mathematical model of a single neuron may demonstrate similar regimes, and variations of certain biophysical parameters in the model can cause transitions between these regimes. These regimes co-exist in certain parameter ranges depending on initial conditions or perturbation. Bursting behavior is well described and has been classified within a framework of the methods of qualitative theory of slow-fast systems; see comprehensive reviews in [17, 27, 28]. Of special interest here are various mechanisms for chaotic bursting analyzed in detail in [2, 24, 32, 34], which occur in transitions from the regime of continuous spikes to bursting. The chaos observed was caused, as is usual, by homoclinic bifurcations of saddle nodes with additional degeneracies, or when such a saddle becomes a saddle-focus with persisting homoclinic structures. Here we report a distinct case in which the bifurcation behind the transition from tonic spiking into bursting is homoclinic but involves a saddle-node periodic orbit instead of saddle equilibria.

A bursting regime reflects complexity in the dynamics of various membrane ionic currents, operating at different time scales. The ionic currents are commonly quantified through voltage-clamp experiments and modelled according to a formalism introduced by Hodgkin and Huxley [15]. A complete neuron model, including all currents identified experimentally, is rather complex for thorough studies.

The relatively small number of neurons in invertebrate nervous systems and possibility to identify most of them from preparation to preparation all make these identifiable neurons attractive for a dynamical system analysis. Here we exploit identified oscillator interneurons that are part of the leech heartbeat central pattern generator.

When isolated pharmacologically from the rest of the network these neurons show autonomous bursting behavior [8]. In these neurons, eight voltage-dependent ionic currents have been identified and characterized, see [14, 25] and references therein. Classified by their ionic specificity, these currents are separated in four groups. The first group consists of two sodium currents: a fast sodium current (I_{Na}) and a persistent sodium current (I_{NaP}). The second group consists of

*Electronic address: ashilnikov@mathstat.gsu.edu
†Also atPhysics Department, Georgia State University, Atlanta, GA 30303, USA

three potassium currents: a delayed rectifier-like potassium current (I_{K1}), a persistent potassium current (I_{K2}) and a fast transient potassium (I_{KA}). The third group consists of two low-threshold calcium currents: one rapidly (I_{CaF}) and one slowly inactivating (I_{CaS}). The last group coexists of a single current, carried by both sodium and potassium: a hyperpolarization-activated current (I_h). All these currents except for the fast sodium current were quantified in voltage clamp experiments, see references in [14]. The model equations for (I_{Na}) were borrowed from the original work by Hodgkin and Huxley adjusted for leech kinetics. None of these currents is dependent on the intracellular concentration of any particular ion. A canonical model of a single neuron has been constructed and tuned to reproduce experimentally observed behaviors [8, 14]. The canonical neuron model is a system of 14 ordinary differential equations running at multiple time scales, varying from a few milliseconds through seconds. As alluded to above a comprehensive analysis of this model would be quite difficult.

Blockade of groups of currents in living heart interneurons simplifies neuronal dynamics, and elicit characteristic behaviors. These characteristic behaviors present interesting phenomena for study from the perspective of the theory of dynamical systems. One of the commonly observed characteristic behaviors is that observed under blockade of Ca^{2+} currents. In leech neurons, application of divalent ions like Co^{2+}, which block Ca^{2+} currents, along with partial block of outward currents, elicit slow plateau-like oscillations with up to 60s period and up to 20 second plateau duration [1, 25]. This phenomenon persists after a blockade of I_h, [25].

Previously, in our modeling studies [7] we addressed the question of how these slow temporal characteristics are produced by a system with dynamics based on much faster time scales (time constants of the ionic currents involved do not exceed one second). We derived a simplified neuron model taking into account that the experimental conditions eliminated or reduced the contribution of certain currents into the dynamics of the neuron. This simplified model, based on the dynamics of I_{Na} and I_{K2} is described as a system of three differential equations. We showed that the classical model of the transient Na^+ current is sufficient for the generation of long plateau behavior due to the properties of a window current (a transient Na^+ current can be a persistent "window" current in a certain range of membrane potential values). The simplified model (1) can produce slow plateau-like oscillations with a sufficiently long plateau phase.

To bring the canonical model developed in [14] in accordance with the experimental conditions described above we remove from the model the equations and terms describing blocked currents: I_{CaF}, I_{CaS}, and I_h. For simplicity, we assume that the partial block of outward currents completely removes I_{K1} and I_{KA}, whereas it reduces I_{K2}. I_{NaP} is removed for simplicity.

Here we employ the model described in [7]:

$$\begin{aligned}
\frac{d\mathrm{V}}{dt} &= -2(\bar{\mathrm{g}}_{\mathrm{K2}}\,\mathrm{m}_{\mathrm{K2}}^2(\mathrm{V}-\mathrm{E}_{\mathrm{K}}) + \mathrm{g}_{\mathrm{l}}\,(\mathrm{V}-\mathrm{E}_{\mathrm{l}}) + \\
&\quad \bar{\mathrm{g}}_{\mathrm{Na}} f(-150, 0.0305, \mathrm{V})^3 \mathrm{h}_{\mathrm{Na}}(\mathrm{V}-\mathrm{E}_{\mathrm{Na}})), \\
\frac{d\mathrm{m}_{\mathrm{K2}}}{dt} &= \frac{f(-83, -0.008, \mathrm{V}) - \mathrm{m}_{\mathrm{K2}}}{\tau_{\mathrm{K2}}}, \qquad (1) \\
\frac{d\mathrm{h}_{\mathrm{Na}}}{dt} &= \frac{f(500, \mathrm{V}_{\mathrm{h}_{1/2}}, \mathrm{V}) - \mathrm{h}_{\mathrm{Na}}}{\tau_{\mathrm{Na}}},
\end{aligned}$$

where the variables V, m_{K2}, and h_{Na} are the membrane potential, activation of I_{K2} and inactivation of I_{Na}, respectively. The parameters are: $\bar{\mathrm{g}}_{\mathrm{K2}}$ is the maximum conductance of I_{K2}; E_{K} and E_{Na} are the reversal potentials of K^+ and Na^+, respectively; $\bar{\mathrm{g}}_{\mathrm{Na}}$ is the maximum conductance of I_{Na}; g_{l} and E_{l} are the conductance and reversal potential of the leak current, respectively; τ_{K2} and τ_{Na} are the time constants of activation of I_{K2} and inactivation of I_{Na}, respectively; $\mathrm{V}_{\mathrm{h}_{1/2}}$ is the membrane potential of half-inactivation of I_{Na}; the function f is given by $f(\mathrm{A}, \mathrm{V}, \mathrm{B}) = 1/(1 + e^{\mathrm{A}(\mathrm{V}+\mathrm{B})})$. The values of the parameters used in this study are $\bar{\mathrm{g}}_{\mathrm{K2}} = 30$ nS, $\mathrm{E}_{\mathrm{K}} = -0.07$ V, $\mathrm{E}_{\mathrm{Na}} = 0.045$ V, $\bar{\mathrm{g}}_{\mathrm{Na}} = 200$ nS, $\mathrm{g}_{\mathrm{l}} = 8$ nS, $\mathrm{E}_{\mathrm{l}} = -0.046$ V, $\tau_{\mathrm{h}_{\mathrm{K2}}} = 0.25$ sec and $\tau_{\mathrm{h}_{\mathrm{Na}}} = 0.0405$ sec. Here (Figs. 1, 8 and 9) we use $\mathrm{V}_{\mathrm{h}_{1/2}}$ as a bifurcation parameter.

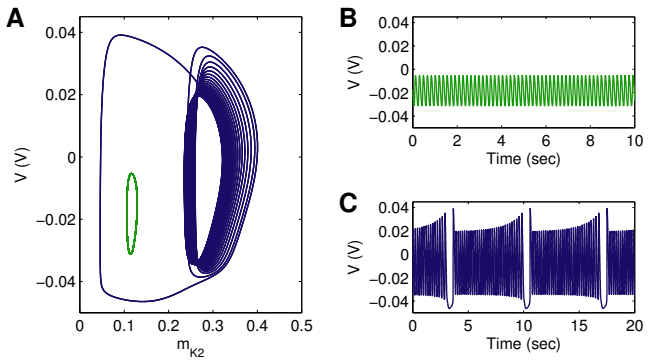

FIG. 1: Co-existence of spiking and bursting modes in the model (1) in the $(\mathrm{V}, \mathrm{m}_{K2})$-projection at the control parameter $\mathrm{V}_{\mathrm{h}_{1/2}} = 0.03367$ V. The initial conditions of the solutions are $(\mathrm{V}, \mathrm{m}_{\mathrm{K2}}, \mathrm{h}_{\mathrm{Na}}) = (0.01048502, 0.10732, 0.06190424)$ and $(-0.03380669, 0.2494588, 0.2866981)$, respectively. The small round periodic orbit in A corresponds to the tonic-spikes shown in B; the larger complex orbit in A corresponds to the bursting cycle shown in C. The topology of this bursting cycle (B) is illustrated in Figs 2 below.

In terms of dynamical systems, co-existence of tonic spiking and bursting corresponds to the co-existence of two distinct attractors in the phase space of the system. Here we describe a codimension-one bifurcation of a saddle-node periodic orbit with noncentral homoclinics, which explains this phenomenon. We present a mechanism for this type of bistability in a general slow-fast 3D system, as well as provide a qualitative understanding for how either attractor can be observed by varying initial conditions. Our analysis explains

also a smooth transition between the regimes. Furthermore, through the analysis we identify physiologically plausible parameters in the model (1) that can control the duration of the burst phase and the number of spikes in a burst. Our results present feasible predictions for experimental studies.

II. PHENOMENOLOGICAL DESCRIPTION

We construct a prototype dynamical system with bifurcational features essential for the phenomenon of bi-stability of tonic spiking and bursting. The principal idea of the construction is based upon a codimension-one bifurcation of a saddle-node periodic orbit with noncentral homoclinics. We show that the bifurcations in our biophysically realistic model are analogous to those in a generic slow-fast $3D$ system of ODEs written in the form:

$$\dot{\mathbf{x}} = F(\mathbf{x}, \alpha) - z, \quad \dot{z} = \mu G(\mathbf{x}, z, \alpha), \tag{2}$$

where $\mathbf{x} = (x, y)$ and z are phase space variables, α is a vector of control parameters, and $0 < \mu << 1$. The function $G(\mathbf{x}, z, \alpha)$ is supposed to be linear in $\mathbf{x}$, and smooth in z. The first restriction is not essential for our analysis and is introduced only for sake of simplicity.

At $\mu = 0$, the *fast* subsystem decouples from the second *slow* one. In this case, the slow variable z becomes a parameter in the fast subsystem. As for the function F, we will require some typical assumptions, like enough smoothness; its essential properties are illustrated in Fig. 2. First, it ensures that the fast subsystem has either one or three equilibrium states, depending on z.

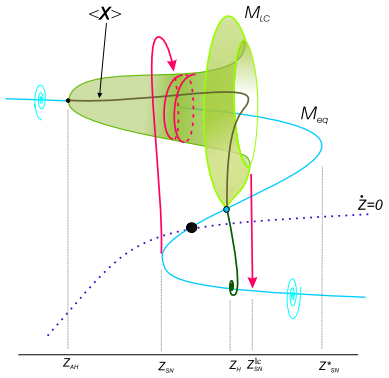

FIG. 2: Bifurcation diagram in the (x, z) plane of the fast subsystem. The red line marks the movement of phase point during bursting projected unto this plane.

The branch $\mathcal{M}_{eq}$ of the equilibria curve for the fast subsystem has a distinctive $\mathcal{Z}$-shape in its projection onto the (z, x)-phase plane. Its equation is given by $z = F(\mathbf{x}, \alpha)$. The two turning points of $\mathcal{M}_{eq}$, at z_{SN} and z^*_{SN}, correspond to the saddle-node bifurcations in the fast subsystem where two equilibrium states coalesce forming a double one. Thus the fast subsystem has three equilibria within the interval $z_{SN} < z < z^*_{SN}$. The middle branch of $\mathcal{M}_{eq}$ is comprised of saddle points. The upper branch of $\mathcal{M}_{eq}$, when stable, corresponds to a depolarized state of the model, whereas the lower one corresponds to a hyperpolarized state. The stable focus on the upper branch $\mathcal{M}_{eq}$ is presumed to become unstable through the supercritical Andronov-Hopf bifurcation at $z = z_{AH}$. This means that the stability of the upper branch of M_{eq} will be imparted, as z increases, onto the parabolic-like surface $\mathcal{M}_{lc}$ composed of limit cycles of the fast subsystem. As z increases further, the forthcoming evolution of the stable limit cycle can follow either of two potential scenarios. In the first case, the stable limit cycle is terminated at the homoclinic bifurcation at some z_H when the saddle point on the middle branch of $\mathcal{M}_{eq}$ has a homoclinic orbit. In addition the saddle value which is the sum of the two characteristic exponents at the saddle point has to be negative. This means that the stable periodic obit may merge into the homoclinic loop. In the second case, which is realized in the considered model, a homoclinic bifurcation also occurs, but the saddle value is *positive*. This means that the unstable limit cycle bifurcates from the homoclinic orbit as z goes through z_H. As z grows further, the stable and the unstable limit cycles get closer, and they merge into a double limit cycle at some z^{lc}_{SN}. This is a saddle-node bifurcation for limit cycles in the fast subsystem. After z^{lc}_{SN} is passed there exists no limit cycle. This scenario makes the surface $\mathcal{M}_{lc}$ look like as being turned inside out, see Figs. 2 and 3.

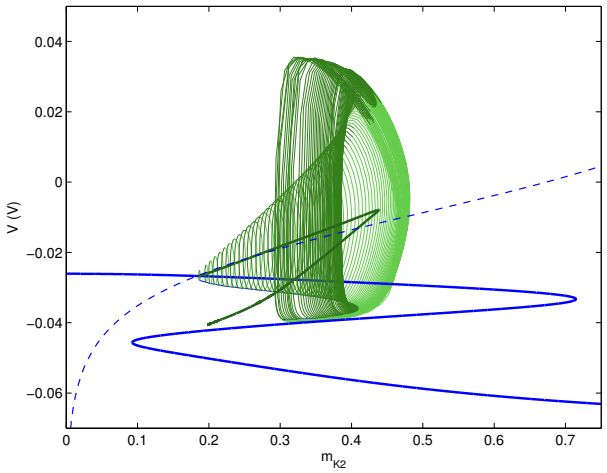

FIG. 3: Slow motion surface in model 1 which is found through continuation of the periodic orbits translated by the nucline $\langle \dot{m}_{K2} \rangle = 0$ (shown dashed). The curve that originate at the Andronov-Hopf bifurcation and terminates at the homoclinic one is the averaged coordinate $\langle V \rangle$ on the periodic orbit vs. $\langle m_{K2} \rangle$. To make it visible the part of the surface adjoining the homoclinic point is not graphed.

After the stable limit cycle disappears for $z > z^{lc}_{sn}$, a nearby phase point moves to another attractor. Such an attractor is a stable equilibrium state on the lower branch of the curve $\mathcal{M}_{eq}$. Now if the parameter z is decreased the phase point will follow the lower branch towards the saddle-node bifurcation at z_{SN}. Then the steady state attractor disappears and the phase point jumps to the stable limit cycle on $\mathcal{M}_{lc}$.

Now that we have described the bifurcation structure of the fast subsystem, let us consider the complete system (II) when $0 < \mu \ll 1$. It follows from the work by Fenichel [10] that when $0 < \mu \ll 1$, the manifold $\mathcal{M}_{eq}$, whenever it is hyperbolic (i.e. far from bifurcations), will persist in the form of some $||\mu||$-close invariant manifold in the singulary perturbed system. Introduce a *null-cline* $G(\mathbf{x}, z, \alpha) = 0$ on which the z-variable does not change, i.e. $\dot{z} = 0$, see Fig. 2. Below $G(\mathbf{x}, z, \alpha) = 0$ the time derivative $\dot{z}$ is negative, while $\dot{z} > 0$ on upper branch of $\mathcal{M}_{eq}$ and the surface $\mathcal{M}_{lc}$. If the above conditions are fulfilled, then the phase point of the 3D system will behave as follows. It drifts slowly along the lower branch of $\mathcal{M}_{eq}$ leftward till the fold. Then it makes a rapid jump up onto the perturbed surface $\mathcal{M}_{lc}$. Afterwards, it drifts slowly rightward in circular motion around $\mathcal{M}_{lc}$. After its z-component passes through the critical value z_{sn}^{lc}, the phase point falls down onto the lower branch $\mathcal{M}_{eq}$, and the cycle starts over again. Such behavior of a trajectory is associated with bursting in neuron models. The number of spikes in a burst is a number of complete revolutions around $\mathcal{M}_{lc}$.

A point where the null-cline crosses $\mathcal{M}_{eq}$ is an equilibrium point in the singularly perturbed system. The coordinates of this point can be found from the system $G(\mathbf{x}, z, \alpha) = 0$ and $F(\mathbf{x}, \alpha) - z = 0$. We presume that null-cline $\dot{z} = 0$ crosses $\mathcal{M}_{eq}$ just once where $\mathcal{M}_{eq}$ represents unstable equilibria.

A. How the smooth transition may occur between tonic spiking and bursting

Let us first discuss the behavior of the trajectories near the surface $\mathcal{M}_{lc}$ in the singularly perturbed system. By construction, the outer surface $\mathcal{M}_{lc}^{s}$ is spanned by the stable limit cycles of the fast system at $\mu = 0$. Define the average value $\langle \mathbf{x} \rangle$ on a such limit cycle $\varphi(t;\, z, \alpha)$ over its period T for a given value of z as follows: $\langle \mathbf{x} \rangle(z, \alpha) = \frac{1}{T(z,\alpha)} \int_0^{T(z,\alpha)} F(\varphi(t;\, z, \alpha), z) dt$. By the construction, the curve $\langle \mathbf{x} \rangle(z)$ originates from the Andronov-Hopf bifurcation at z_{AH} and terminates at the homoclinic bifurcation at z_{sn}^{lc} as described above. Note that the curve has a distinctive fold where the stable and unstable limit cycles coalesce (Fig. 2). Thus, in terms of the Pontryagin averaged fast subsystem, its equilibrium state corresponds to a limit cycle in the fast subsystem and the fold corresponds to the saddle-node bifurcation of limit cycles.

Note that the Fenichel theory holds true also for the normally hyperbolic branch of $\langle \mathbf{x} \rangle$ outside the fold and the Andronov-Hopf points.

The corresponding averaged slow subsystem is given by

$$\begin{aligned} \dot{z} &= \mu \tilde{G}(\langle \mathbf{x} \rangle, z, \alpha), \\ \tilde{G} &= \frac{1}{T(z,\alpha)} \int_0^{T(z,\alpha)} G(\varphi(t;\, z, \alpha), z)\, dt, \end{aligned} \tag{3}$$

It is defined on the slow manifold, denoted by $\langle \mathbf{x} \rangle$ corresponding to equilibria of the averaged fast subsystem. Note that the upper segment of $\langle \mathbf{x} \rangle$ linking the Andronov-Hopf and fold bifurcation points consists of the stable equilibria of the averaged subsystem. Its lower segment between the fold and homoclinic bifurcation points consists of the repelling equilibria which are the images of the unstable limit cycles.

Suppose next that the upper branch of $\langle \mathbf{x} \rangle$ is crossed transversally by the null-cline $\langle \dot{z} \rangle = 0$. The intersection point is an equilibrium state of the averaged system. The equilibrium state will be stable if the curve crosses $\langle \mathbf{x} \rangle$ from below, and unstable in z otherwise. The stable equilibrium state of the averaged system is the image of the stable periodic orbit in the 3D singularly perturbed system, see Figs. 4,5. This stable periodic orbit corresponds to periodic tonic spiking activity of a neuron model.

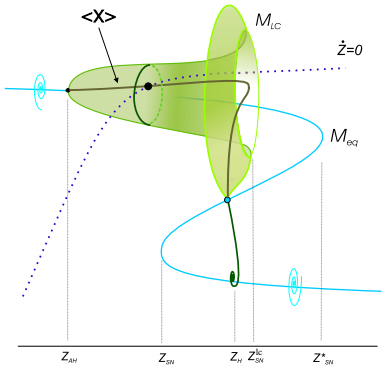

FIG. 4: Stable periodic orbit at the transverse intersection of the null-cline $\langle \dot{z} \rangle = 0$ with the curve $\langle \mathbf{x} \rangle$.

When the surface $\langle \dot{z} \rangle = 0$ is crossed by the curve $\langle \mathbf{x} \rangle$ twice, then the intersection points will correspond to the two periodic orbits, one stable and one of the saddle type, see Fig. 5. They correspond to the stable and saddle periodic orbits on (or about) the surface $\mathcal{M}_{lc}$ in the whole 3D system. Here, of a very special interest is an interplay between the stable manifold of the saddle periodic orbit that is shown as a grey disk in this figure, and the way the phase point jumps up at $\sim z_{sn}$ (the left fold on the Z-shape curve of equilibria of the fast subsystem) onto the surface $\mathcal{M}_{lc}$. Two robust situations are possible here. The first shown in Fig. 5(a) is when the phase point gets, once or after some intermediate phase, into the attraction basin of the stable periodic orbit. Then, the system will generate tonic spikes as shown by numerical simulations of system 1 in Fig. 8. In the second case illustrated in Fig. 5(b), the stable manifold of the unstable cycle does separate the attraction basin of the stable periodic orbit. This corresponds to the bi-stability in the system, where the the tonic-spike solution co-exists with the bursting solution, see the numerical results presented in Fig. 1. The choice of the regime is determined by the initial condition.

The periodic orbits merge when t $\langle \dot{z} \rangle = 0$ becomes tangent to $\langle \mathbf{x} \rangle$. The point of the contact corresponds to the saddle-node periodic orbit in the phase space of the 3D singularly perturbed system [30]. This orbit vanishes as $\langle \dot{z} \rangle = 0$ moves below $\langle \mathbf{x} \rangle$. Therefore, there is no bi-stability after the saddle-node bifurcation in the system which starts firing bursts only.

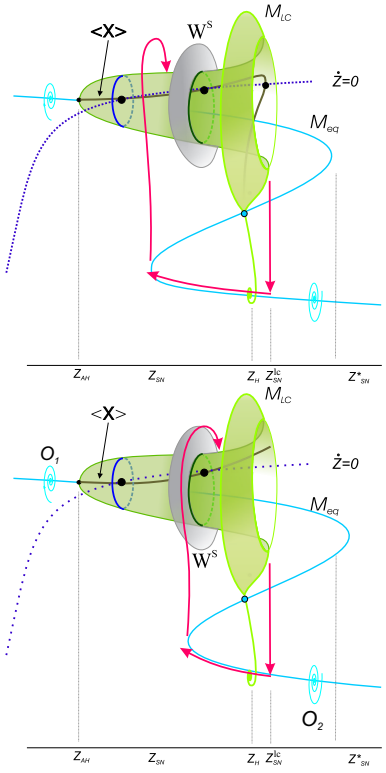

FIG. 5: (A) Points of transverse intersections of $\langle \dot{z} \rangle = 0$ with $\langle \mathbf{x} \rangle$ are the images of the two periodic orbits: one stable and one saddle in the phase space of the 3D singularly perturbed system. This corresponds to Inset 2 in Fig. 7. (B) Bi-stability starts when the stable manifold of the saddle periodic orbit bounds the attraction basin of the stable orbit. This situation corresponds to Inset 4 in Fig. 7.

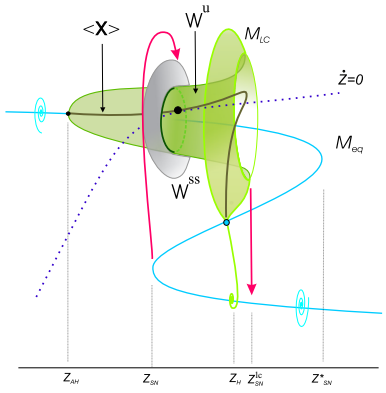

FIG. 6: Tangency between $\langle \dot{z} \rangle = 0$ and $\langle \mathbf{x} \rangle$ generates a saddle-node periodic orbit. Its 2D unstable manifold W_u comes back to the bifurcating periodic orbit L_{sn} along its strongly stable manifold W^{ss}.

In the following section we discuss the mechanisms that give rise to this bistability and are behind the onset of chaos in the system. They are related to homoclinic bifurcations involving the saddle periodic orbit and the saddle-node periodic orbit at the critical moment.

III. NONCENTRAL SADDLE-NODE BIFURCATION

The codimension of a local saddle-node periodic orbit bifurcation is one but it can be higher depending upon the global properties of the 2D unstable manifold of the saddle-node periodic orbit. Following Shilnikov et al. [30] we shall identify a strongly stable (also called non-leading) manifold W^{ss}_{sn} of the bifurcating periodic orbit L_{sn}. This manifold is homeomorphic to the disk-like one shown in Fig. 7. This manifold separates the saddle region (to the right of it) from the node region (to the left). A trajectory originating in the node region tends to the saddle-node periodic orbit as time $t \to +\infty$. The unstable manifold W^u_{sn} of the saddle-node periodic orbit is a semi-cylinder μ-close to a part of $\mathcal{M}_{lc}$ on the right of W^{ss} such that a trajectory starting on W^u tends to the periodic orbit as $t \to -\infty$. We are interested in how the unstable manifold of the periodic orbit may return to L_{sn} as $t \to +\infty$. In this paper, we consider a special case where W^u returns to the saddle-node orbit along its strongly stable manifold W^{ss}. Note that since a generic intersection of two surfaces is transverse in R^3, the given bifurcation remains of the codimension one.

This bifurcation was first introduced and studied by Lukyanov and Shilnikov [21]. Let us elaborate on its essential features. An unfolding of the bifurcation is sketched in Fig. 7.

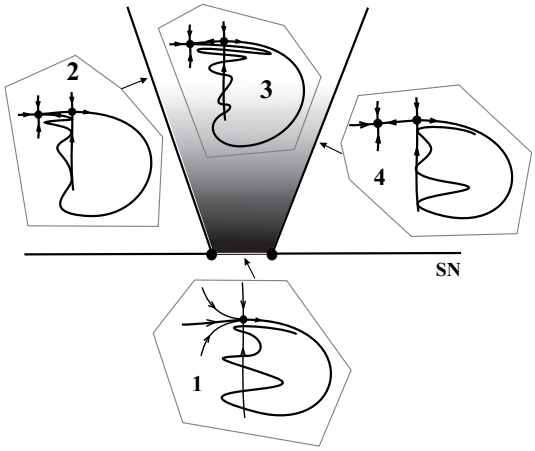

FIG. 7: There are 3 principal bifurcation curves in the unfolding for the Lukyanov-Shilnikov bifurcation of a saddle-node fixed point with non-central homoclinics (inset 1). The two bifurcation curves, which are the boundaries of the darkened sector, correspond to the very first (inset 2) and last (inset 4) homoclinic tangencies between the stable and unstable manifolds of the saddle fixed point. The complex hyperbolic structure existing in this wedge, is due to transverse homoclinic crossings (inset 3). This structure will persist after disappearance of the saddle-node point below the corresponding bifurcation (horizontal) line SN.

It is convenient to describe the bifurcation sequence using a two-dimensional Poincaré map defined on some cross-section transverse to the periodic orbits. This cross-section can be a fragment of a plane parallel to the (x, z)-plane. A point where a periodic orbit hits the cross-section is a fixed point of the Poincaré map. The stability of the point is the same

as that of the periodic orbit. In the case of the saddle-node periodic orbit, there is a single fixed point of the saddle-node type. In the case when the double periodic orbit splits into the two periodic orbits, the corresponding fixed point splits into one stable and one saddle type fixed point. Moreover, because the saddle-node fixed point has non-central homoclinic orbits generated by transverse crossings of its unstable and strongly stable manifolds, it follows that after the splitting, the saddle point inherits the transverse homoclinic structure.

Let ε be a single vector controlling the distance between the fixed points so that there is none when $\varepsilon > 0$. Let U be a small neighborhood containing the double fixed point (periodic orbit) with the homoclinic orbit, and let $\Omega_U(\varepsilon)$ denote the set of all trajectories lying entirely in U except for the stable orbit when $\varepsilon < 0$. Then we have the following two theorems.

Theorem 1 [Lukyanov-Shilnikov] *There exist a small neighborhood U of the origin and $\varepsilon_1 < 0$ such that for all $\varepsilon \in [\varepsilon_1, 0]$ the set $\Omega_U(\varepsilon)$ is homeomorphic with suspension over the Bernoulli subshift on two symbols.*

Theorem 2 [Lukyanov-Shilnikov] *There exists a neighborhood U, $\bar{\varepsilon} > 0$ and a partition of the interval $(0, \bar{\varepsilon}]$*

$$0 < \cdots < \varepsilon_{k+1+\bar{k}} < \varepsilon'_{k+1+\bar{k}} < \varepsilon_{k+\bar{k}} < \cdots < \varepsilon_{\bar{k}} = \bar{\varepsilon},$$

such that for $\varepsilon \in (\varepsilon_{k+1+\bar{k}}, \varepsilon_{k+\bar{k}}$ the set $\Omega_U(\varepsilon)$ contains an invariant subset $\Omega^k_U(\varepsilon)$ homeomorphic with the suspension over a Bernoulli subshift on $\bar{k} + k$ symbols, while $\Omega_U(\varepsilon)$ is homeomorphic with $\Omega^k_U(\varepsilon)$ for $\varepsilon \in (\varepsilon'_{k+1+\bar{k}}, \varepsilon_{k+\bar{k}}$. As $\varepsilon to 0$ there arises an infinite set of bifurcation connected with the appearance of Smale horseshoes.

In other words, the system possesses a complex shift-dynamics above SN within the wedge bounded by two curves corresponding to the very first and last contacts between the stable and unstable manifolds of the saddle fixed point (periodic orbit) and below it. This dynamics is associated with the existence of the Smale horseshoes at the transverse intersections of the stable and unstable manifolds of the saddle-fixed point. As the fixed point disappears through the saddle-node bifurcation, the hyperbolic subset nevertheless persists. The presence of the Smale horseshoes in the phase space of the whole system results in complex chaotic dynamics which can be observed in a vicinity of the just disappeared fixed point. There arise also some other relevant complex phenomena such as Newhouse regions of dense structural instability which are due to homoclinic tangencies of the manifolds, see [11, 12], which are far beyond the scope of this work.

A. Lukyanov-Shilnikov bifurcation in the neuron model

Let us now apply these results to our neuronal model and its phenomenological reflection. Let us look again at the inset 2 in Fig. 7. Here there are two fixed points. The attraction basin of the stable point is such that almost any trajectory converges to this sole attractor. In terms of the flow, the corresponding situation is depicted in Fig. 5(a) where the unstable manifold of the saddle periodic orbit does not separate the "bursting" mode from the tonic spiking mode. So, as soon as the phase point moves from the hyperpolarized state it gets attracted by the stable periodic orbit. Thus, the neuron will tonically generate spikes like ones shown in Fig. 8.

The region corresponding to inset 3 in Fig. 7 features a chaotic saddle. The attractor is again the stable fixed point of the map and the stable periodic orbit in Fig. 8. Although the chaotic regime is not attractive, there is chaos in the system in the sense that the number of bursts before switching to tonic spiking sensitively depends on the initial point, i.e. it may vary from 1 up to infinity. Here, Fig. 8, the neuron fires a sequence of four bursts before switching to the tonic spiking regime.

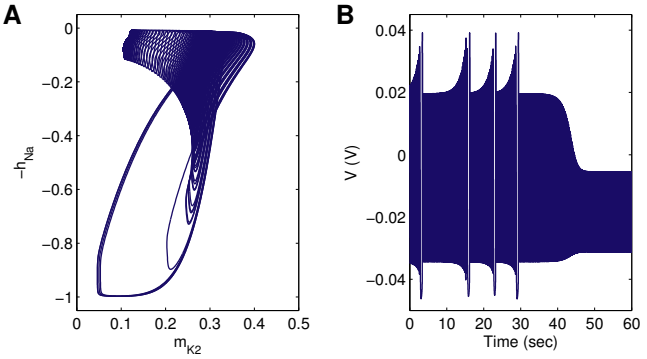

FIG. 8: Intermittent transition to tonic spiking, such that a number of bursts is generated before the stable periodic orbit captures the phase point presented in a projection on the $-\mathrm{h}_{Na}$ and m_{K2} plane (A) and as a voltage-time series (B). This intermittency corresponds to region (3) in Fig. 7. The model (1) is at control parameter $\mathrm{V}_{\mathrm{h}_{1/2}} = 0.03367$ V.

In the region (4) the neuron is bi-stable, i.e. depending on the initial conditions it can generate either tonic spiking or busting . The bi-stability forms when the stable manifold of the saddle fixed point bounds the attraction domain of the stable fixed point in Fig. 7, or in in terms of the flow, when the unstable manifold of the saddle periodic orbit separates the attraction domain of the stable periodic orbit, see Fig. 5(b). It is interesting to note that the bursting oscillations can be of two types: regular (periodic) or irregular (chaotic) compare Figs. 1 and 9. The chaotic bursting is observed for the parameter values close to the corresponding boundary (like the boundary between the regions 3 and 4 in Fig. 7), according with results obtained in [11].

After both periodic orbits disappear through the saddle-node bifurcation only the bursting mode will persist. It can be either chaotic or periodic. This depends on whether the hyperbolic set still exists in the region right beneath the corresponding bifurcation curve SN. Away from SN the bursting becomes regular.

IV. CONCLUSION

We have described a mechanism for the transition between tonic spiking and bursting. This mechanism also explains

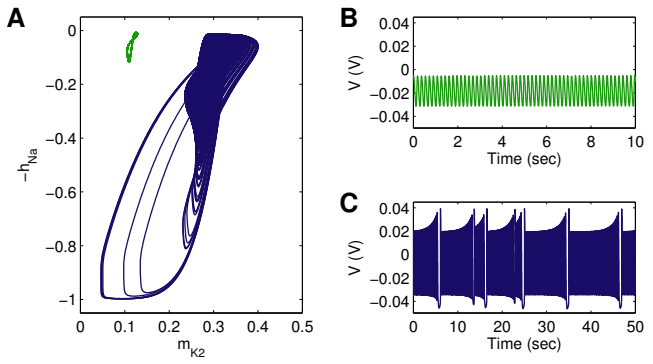

FIG. 9: Chaotic bursting at $\mathrm{V_{h_{1/2}}} = 0.0336709$ V presented in a projection on the $(-\mathrm{h}_{Na}, \mathrm{m}_{K2})$ plane (A) and as a voltage-time series (B). Adjusting $\mathrm{V_{h_{1/2}}}$ regularizes bursting as shown in Fig. 1.

possible bi-stability in the system, where bursting mode coexists with tonic spiking and a particular mode can be attained by appropriate choice of initial conditions. The core of the mechanism is based on a bifurcation of codimension one for a saddle-node periodic orbit with non-central homoclinic orbits.

For the first time this bifurcation has been shown to occur in a autonomous model describing the dynamics of a physical entity. Moreover, we argue that the scenario and the geometry of the bifurcation are both quite typical for fast-slow systems based on the Hodgkin-Huxley formalism.

The averaging method used for locating the periodic orbits in the *whole* (not only fast) system provides a powerful geometrical tool for the analysis of the global bifurcations. This method utilizes essentially an interaction dynamics between the slow and fast sub-systems which was not fully exploited in previous studies.

V. ACKNOWLEDGMENT

We thank D. Turaev for his helpful comments. The numeric analysis of system (1) utilized the software packages CONTENT and MATCONT [9]. A.S. acknowledge the RFBR grants No. 02-01-00273 and No. 01-01-00975. G.C. and R.L.C. were supported by NIH grants NS43098.

[1] J. Angstadt and W. Friesen, J. Neurophysiol. **66**, 1858 (1991).
[2] V.N. Belykh, I.V. Belykh, M. Colding-Joregensen, E. Mosekilde, Eur. Phys. J. **3**, 205, (200).
[3] R. Bertram, Biol. Cybern. **69** 257 (1993).
[4] R. Butera, Chaos **8** 274 (1998).
[5] C.C. Canavier, D.A. Baxter, L. Clark, J. Byrne. J. Neurophysiol. **69**, 2252 (1993).
[6] C.C. Canavier, D.A. Baxter, J. Clark, J. Byrne, J. Neurophysiol. **72** 872 (1994).
[7] G.S. Cymbalyuk and R.L. Calabrese. Neurocomputing, 159 (2001).
[8] G.S. Cymbalyuk, Q. Gaudry, M.A. Masino, R.L. Calabrese J. Neuroscience **22**, 10580, 2002.
[9] A. Dhooge, W. Govaerts, Yu.A. Kuznetsov, ACM Trans. Math. Software **29**, 141 (2003)
[10] N. Fenichel, J. Diff. Eq. **31** 53 (1979)
[11] N.F. Gavrilov, L.P. Shilnikov, Math. USSR Sb. **17**, 467 (1972), **19**, 139 (1973).
[12] S. Gonchenko, L.P.Shilnikov and D.V.Turaev, Physica D **62**, 1, 1993.
[13] J. Hartings, S. Temereanca, D. Simons, J. Neuroscience **23** 5264 (2003).
[14] A. Hill, J. Lu, M. Masino, O. Olsen, R.L. Calabrese, J. Comput. Neuroscience **10**, 281 (2001).
[15] A.L. Hodgkin, A.F. Huxley, J. Physiol. **117**, 500 (1952).
[16] J. Hounsgaard, O. Kiehn, J. Physiol. **414**, 265 (1989)
[17] E. Izhikevich, J. Bifurcation and Chaos **10**(6), 1171, (2000)
[18] E. Izhikevich, N. Desai, E. Walcott, F. Hoppensteadt, Trends Neurosci. **26** 161 (2003).
[19] H. Lechner, D. Baxter, C. Clark, J. Byrne, J. Neurophysiol. **75** 957 (1996).
[20] J. Lisman (1997) Trends Neurosci. **20**, 38 (1997).
[21] V. Lukaynov and L. Shilnikov, Soviet Math. Dokl. **19**(6), 1314 (1978)
[22] E. Marder, L. Abbott, G. Turrigiano, Z. Liu, J. Golowasch, Proc. Natl. Acad. Sci. USA **26-93**(24), 13481 (1996).
[23] E. Marder , R.L. Calabrese, Physiol. Rev. **76**, 687 (1996).
[24] E. Mosekilde, B. Lading, S. Yanchuk, Yu. Maistrenko, Biosystems, **63** 3 (2001).
[25] C.A. Opdyke and R.L. Calabrese, J. Comp. Physiol. *175*, 781 (1994).
[26] P. Reinagel, D. Godwin, S.M. Sherman, C. Koch, J. Neurophysiol. **81**, 2558, 1999
[27] J. Rinzel, Lecture Notes in Mathematics **1151**, 304 (1985)
[28] J. Rinzel, Lecture Notes in Biomathematics **71**, 267 (1987).
[29] A. Shilnikiov, L. Shilnikov and D. Turaev, Moscow Math. Journal (2004) to appear.
[30] L. Shilnikov, A. Shilnikiov, D. Turaev and L. Chua Methods qualitative theory in nonlinear dynamics, Volumes I and II. World Scientific, (1998 and 2001)
[31] M. Steriade, D.A. McCormick, T.J. Sejnowski, Science **262**, 679, 1993.
[32] D. Terman, J. Nonlinear science **2**, 135 (1992).
[33] G. Turrigiano, E. Marder, L. Abbott, J. Neurophysiol. **75** 963 (1996).
[34] X.J. Wang, Physica D **62**, 263 (1993).
[35] X.J. Wang, Neuroscience **59**(1), 21 (1994).